International Journal of Engineering and Advanced Technology (IJEAT)
ISSN: 2249-8958 (Online), Volume-4 Issue-4, April 2015

Robust Stabilization of Single Area LFC Loop through Extended State Observer

Rittu Angu, R. K. Mehta

Abstract: ***An Extended State Observer (ESO) based design approach has been presented for a Load Frequency Control (LFC) loop of a single area. The design approach utilizes the full state feedback as well as an estimated signal for parameter uncertainty and disturbances due to load demand changes to form the control law. The ESO-based design approach is capable of estimating state as well as disturbances together in order to compensate system in presence of parameter uncertainty and disturbances due to load demand changes. The proposed design methodology achieves performance satisfying the specified stability margins. The methodology provides a control over peak values of the frequency and control signal deviations which may be utilized to meet hardware constraints. An illustrative example illustrates the effectiveness of the developed methodology.***

Keywords: Load frequency control, Control area, extended state observer, augmented system, MATLAB simulation.

I. INTRODUCTION

The modern power systems with industrial and commercial loads need to operate at constant frequency with reliable uninterrupted power. However, it is not possible for a system to remain in steady state, since the load demands keeps on changing all the time with rising or falling trend. Steam input to the steam-turbine and water input the hydro-generator must therefore be continuously regulated to match the active power demand, failing which the frequency (machine speed) will vary[6]. A well designed power system should therefore be able to provide the acceptable levels of power quality by keeping the frequency and voltage magnitude within tolerable limits. However, the users of the electric power change the loads randomly and momentarily. Thus, a control system is essential to cancel the effects of the random load changes and to keep the frequency and voltage at the standard values. Changes in the power system load affect mainly the system frequency, while the reactive power is less sensitive to changes in frequency and is mainly dependent on fluctuations of voltage magnitude [5]. So the control of the real and reactive power in the power system is dealt separately. The load frequency control mainly deals with the control of the system frequency and real power whereas the automatic voltage regulator loop regulates the changes in the reactive power and voltage magnitude. Load frequency control is the basis of many advanced concepts of the large scale control of the power system.

Manuscript published on 30 April 2015.
* Correspondence Author (s)
Rittu Angu, M-Tech in Power System Engineering in 2013 from NERIST (Deemed University), Nirjuli Itanagar, India.
Dr. R. K. Mehta, Assoc. Prof., Department of Electrical Engineering, NERIST, Nirjuli, Arunachal Pradesh, India.

The present work attempts to utilize an ESO-based full state feedback for single area load frequency control design. The control objective is to develop a procedure for designing state feedback for a given plant conditions; the specifications set as:
(i) No deviation in frequency in steady-state for a step change in load demand.
(ii) Critical gain and phase margins must be greater or equal to the specified GM and PM.
It is assumed that the load frequency model parameters (i.e. R, T_H, T_T, T_p and K_p) are given, output frequency is available for feedback. State feedback has potential to improve the performance of the load frequency by judicious choice of closed-loop pole locations. An extended state observer has been constructed to meet the performance requirements and iterative design steps are required to ensure satisfactory operation. The LFC model incorporates ESO-based design for improved command tracking and to enhance disturbance rejection capability for the proposed control scheme. Moreover, a realistic LFC system having uncertain variations in parameters from the nominal values will be characterized by deviations in the nominal values of LFC parameters (T_H, T_T, T_p, H and D).

In this paper, the parametric model uncertainty has been considered, which represents imprecision of the parameters within the model. The ESO-based closed-loop plant stability robustness studies have been carried out assigning a bound on the deviations in LFC system. Numerical results are presented to demonstrate the efficacy of the proposed control design procedure and to evaluate the performance and robustness qualities of the controller.

II. PLANT MODEL

A single area power system shown in Figure 1 consists of a governor, a turbine and a generator with feedback of regulation constant R. System also includes step load change (ΔP_D) input to the generator. Where $G_H(s)$, $G_T(s)$ and $G_P(s)$ are open-loop transfer functions of each unit. The state variable model for the open-loop system [1] is

$$\dot{x} = Ax + Bu$$
$$y = Cx \qquad (1)$$

With disturbance w Equation (1) reduces to

$$\dot{x} = Ax + Bu + B_1 w$$
$$y = Cx \qquad (2)$$

The state variables are chosen as

Published By:
Blue Eyes Intelligence Engineering
and Sciences Publication (BEIESP)

$$x = \begin{bmatrix} x_1 \\ x_2 \\ x_3 \end{bmatrix} = \begin{bmatrix} \Delta P_V \\ \Delta P_T \\ \Delta f \end{bmatrix}$$

The state model of open-loop LFC system with output as frequency Δf (from Equation 2) becomes

$$\dot{x} = \begin{bmatrix} -\frac{1}{T_H} & 0 & -\frac{1}{RT_H} \\ \frac{1}{T_T} & -\frac{1}{T_T} & 0 \\ 0 & \frac{K_P}{T_P} & -\frac{1}{T_P} \end{bmatrix} \begin{bmatrix} x_1 \\ x_2 \\ x_3 \end{bmatrix} + \begin{bmatrix} \frac{1}{TH} \\ 0 \\ 0 \end{bmatrix} u + \begin{bmatrix} 0 \\ 0 \\ -\frac{K_P}{T_P} \end{bmatrix} w$$

$$y = [0\ 0\ 1]x \qquad (3)$$

where $u = [\Delta P_g]$, $w = [\Delta P_D]$

The LFC model in the open-loop has three real poles ($-\frac{1}{T_H}, -\frac{1}{T_T}$ and $-\frac{1}{T_P}$) determined by the time constants of governor (hydraulic system), turbine and generator transfer functions models [1]. The system (A, B) is completely controllable. The proposed closed-loop control scheme for achieving desired transient and steady-state performance is discussed in the preceding section.

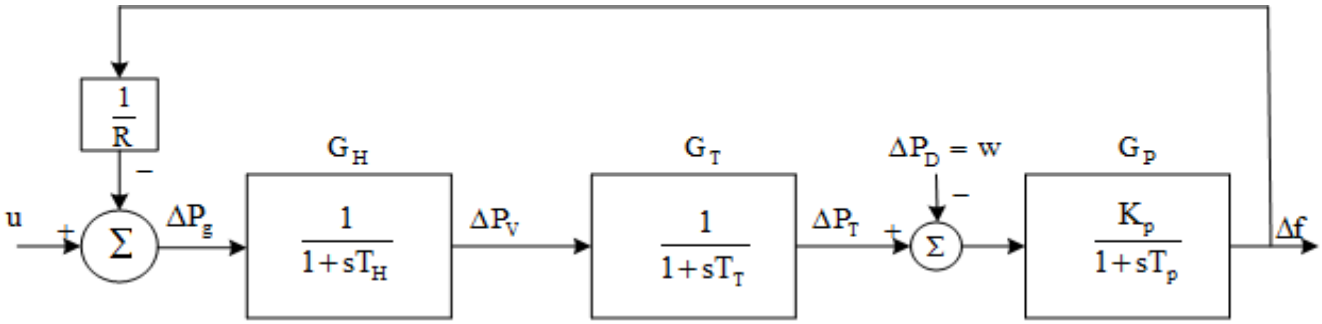

Figure 1: Model of a single area power system.

III. ESO BASED CONTROL SCHEME

Figure 2 shows the full state feedback scheme based on an extended state observer (ESO). The open-loop LFC static model with system frequency (Δf) as output is given by Equation (1).

Where $x = [x_1\ x_2\ x_3]^T$ and matrices A, B, C and B_1 defined by Equation (3).

The ESO measures the disturbance w due to load changes. It is assumed that the state variablesx_1 (ΔP_V), x_2 (ΔP_T) and x_3(Δf) are to be estimated to eliminate the need for three sensors. So, the extended observer in Figure (2) is to be designed as fourth order system to provide estimated variables $\hat{x}_1, \hat{x}_2, \hat{x}_3$ and $\hat{w}$.

The state feedback gains (k_1, k_2 and k_3) are determined by pole-placement technique. The controller poles (closed-loop) have been decided considering the stability margin at X (shown in Figure 2).

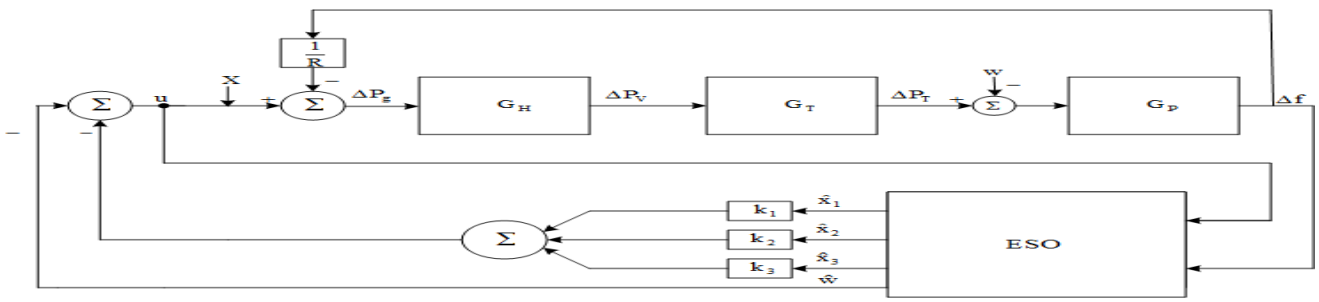

Figure 2: Closed-loop control scheme with ESO in feedback loop.

Published By:
Blue Eyes Intelligence Engineering
and Sciences Publication (BEIESP)

IV. EXTENDED STATE OBSERVER DESIGN

The extended order observer (ESO) design [7] has been carried out assuming a constant unknown disturbance appearing at the generator input. Then, the disturbance dynamic can be given by $\dot{w} = 0$, resulting in A_d=0 and C_d=1. Combining the plant with disturbance generator, the augmented plant in the state-space model is

$$\dot{x}_a = A_a x_a + B_a u$$
$$y = C_a x_a \qquad (4)$$

Where $x_a = [\, x_1 \;\; x_2 \;\; x_3 \;\; w \,]^T$. The matrices are

$$A_a = \begin{bmatrix} -\frac{1}{T_H} & 0 & -\frac{1}{RT_H} & \frac{1}{T_H} \\ \frac{1}{T_T} & -\frac{1}{T_T} & 0 & 0 \\ 0 & \frac{K_p}{T_p} & -\frac{1}{T_p} & 0 \\ 0 & 0 & 0 & 0 \end{bmatrix}, \; B_a = \begin{bmatrix} \frac{1}{T_H} \\ 0 \\ 0 \\ 0 \end{bmatrix}, \; C_a = \begin{bmatrix} 0 & 0 & 1 & 0 \\ 0 & 0 & 0 & 0 \\ 0 & 0 & 0 & 0 \\ 0 & 0 & 0 & 0 \end{bmatrix}$$

If the pair (A_a, C_a) is observable and if system (A_a, B_a, C_a) does not have a zero, Equation (4) will be observable and an observer can be constructed that will compute the estimates for x_1, x_2 and x_3 of plant and w. If form ($-\hat{w}$) is added to the control (Figure 2), then it will cancel out the effects of the real disturbance.

To construct third-order observer, the compatible transformation matrix on the basis of the augmented system (Equation 4) is introduced by

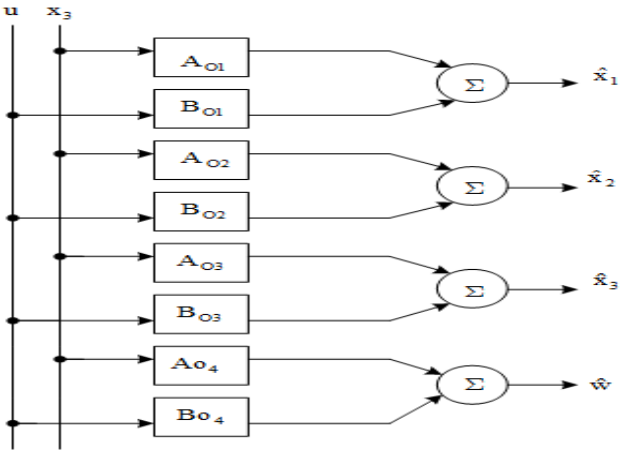

Figure 3: 4th order extended state observer.

$$z = Tx_a = \begin{bmatrix} t_{11} & t_{12} & t_{13} & t_{14} \\ t_{21} & t_{22} & t_{23} & t_{24} \\ t_{31} & t_{32} & t_{33} & t_{34} \\ t_{41} & t_{42} & t_{43} & t_{44} \end{bmatrix} x_a \qquad (5)$$

Where T is the 4x4 matrix and z is the 4x1 matrix. The fourth-order observer driven by x_3 and u, but the control has additional form $(-\hat{w})$.

$$\dot{z} = Dz + Fx_a + Gu$$
$$u = -(k_1\hat{x}_1 + k_2\hat{x}_2 + k_3\hat{x}_3) - \hat{w} + r$$

Where

$$z = [z_1 \;\; z_2 \;\; z_3 \;\; z_4]^T$$

$$D = \begin{bmatrix} 0 & 1 & 0 & 0 \\ 0 & 0 & 1 & 0 \\ 0 & 0 & 0 & 1 \\ -d_0 & -d_1 & -d_2 & -d_3 \end{bmatrix}$$

$$F = \begin{bmatrix} 0 & 0 & 0 & 1 \\ 0 & 0 & 0 & 0 \\ 0 & 0 & 0 & 0 \\ 0 & 0 & 0 & 0 \end{bmatrix}$$

The Luenberger's compatibility conditions to be satisfied [4] in the design of the observer are

$$TA - DT = F \qquad (6)$$

$$G = TB_a \qquad (7)$$

As a rule of thumb, the observer poles can be chosen to be faster than the controller poles by a factor of 2 to 7 [8], the third pole (real) of the observer due to disturbance dynamic has been placed such that the stability margins are satisfied.

Thus, for known values for A and D matrices, T-matrix is obtained from Equation (6) using MATLAB program. Using Equation (7),

$$G = TB_a = \begin{bmatrix} t_{11}/T_H \\ t_{21}/T_H \\ t_{31}/T_H \\ t_{41}/T_H \end{bmatrix}$$

Thus, the estimation of x_1, x_2, x_3 and w denoted as $\hat{x}_1, \hat{x}_2, \hat{x}_3$ and $\hat{w}$ respectively can be obtained by rewriting the equation in the form shown below

$$\hat{x}_a = Mz \qquad (8)$$

$$M = T^{-1} = \begin{bmatrix} m_{11} & m_{12} & m_{13} & m_{14} \\ m_{21} & m_{22} & m_{23} & m_{24} \\ m_{31} & m_{32} & m_{33} & m_{34} \\ m_{31} & m_{32} & m_{33} & m_{44} \end{bmatrix} \qquad (9)$$

From the light of above equations and Figure 2, block diagram of Figure 4 is drawn.

V. CLOSED-LOOP POLE LOCATIONS

The main objective of optimal regulator or controller design known as linear quadratic regulator (LQR) is to define the performance index (cost function) J and search for u=-Kx that minimizes this index to stabilize the system (i.e. to transfer the system from its initial state to final state such that a given performance index is minimized).

Published By:
Blue Eyes Intelligence Engineering
and Sciences Publication (BEIESP)

The objective is to find the feedback K of control law such that the performance index

$$J = \int_0^\infty \rho y^2(t) + u^2(t)dt$$

is minimized for the system (A, B). Here the optimal value of K is that which places the closed poles at the stable roots of the symmetric root locus equation [3]

$$1 + \rho G(-s)G(s) = 0 \qquad (10)$$

In standard form

$$1 + \rho \frac{N(-s)N(s)}{D(-s)D(s)} = 0$$

Where G(s) is the open loop transfer function

$$G(s) = \frac{y(s)}{u(s)} = \frac{N(s)}{D(s)} = C(SI - A)^{-1}B$$

and ρ represent weighting penalties on the state variables and control inputs and is chosen by the designer. The controller's performance highly depends on the choice of the weighting factor ρ. Wrong choice of this may result to the frequency and power oscillating during disturbances. In reality, choosing different values of ρ can provide us with pole locations that achieve varying balances between a fast response and a low control effort. In practice, usually a value of ρ corresponding to a point close to the knee of the trade-off curve is chosen. This is because it provides a reasonable compromise between the use of control and the speed of response.

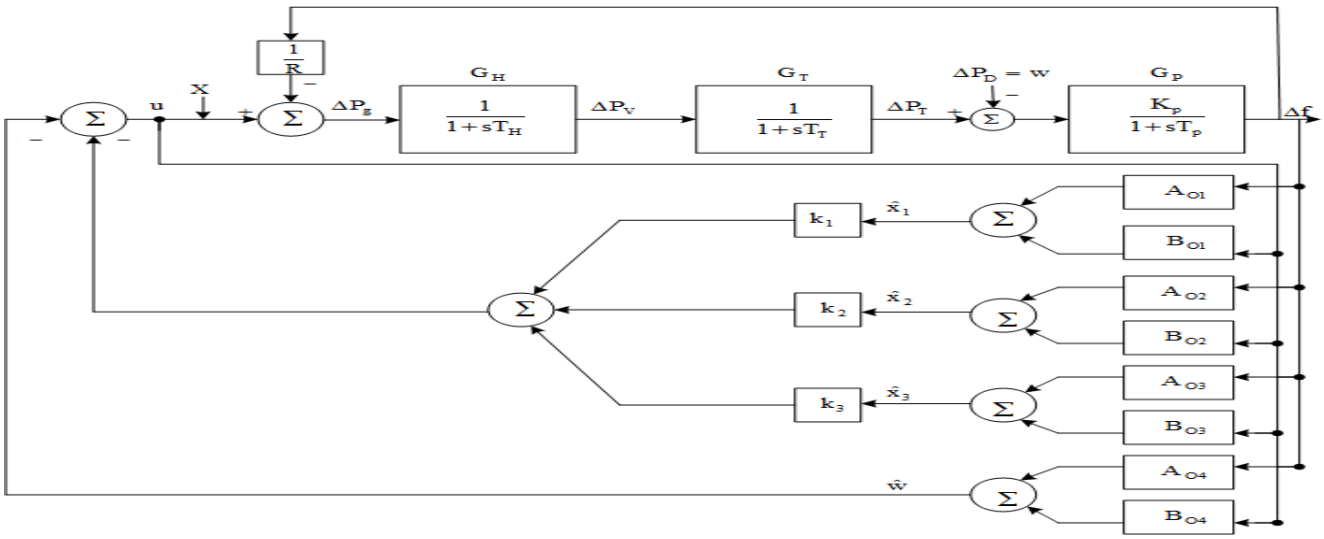

Figure 4: Closed-loop system with ESO in transfer function models.

VI. STABILITY ANALYSIS

The open loop transfer function of the proposed system is obtained by opening its forward path and is solved by Mason's Gain formula for signal flow graph [2]. We consider the loop marked X in Figure 4 in our design approach to establish the stability margin in terms of open-loop gain responses. This is in-fact the ability of proposed system to deal successfully in-case of model uncertainties. The system is stable when gain values are increased but it may become unstable if the gain increases past a certain critical limit. The transfer function of open loop at X is

$$G_x(s) = \frac{N_4 s^3 + N_3 s^2 + N_2 s + N_1}{D_8 s^7 + D_7 s^6 + D_6 s^5 + D_5 s^4 + D_4 s^3 + D_3 s^2 + D_2 s + D_1} \qquad (11)$$

$$N_4 = (Rg_{o3}k_p + Ra_{o3}k_1k_p + Rc_{o3}k_2k_p + Re_{o3}k_3k_p), N_3 = (Rg_{o2}k_p + Ra_{o2}k_1k_p + Rc_{o2}k_2k_p + Re_{o2}k_3k_p)$$

$$N_2 = (Rg_{o1}k_p + Ra_{o1}k_1k_p + Rc_{o1}k_2k_p + Re_{o1}k_3k_p), N_1 = (Rg_{o0}k_p + Ra_{o0}k_1k_p + Rc_{o0}k_2k_p + Re_{o0}k_3k_p)$$

$$D_8 = Rh_3$$

$$D_7 = Rh_2 + Rh_3(d_3 + h_{o3} + b_{o3}k_1 + d_{o3}k_2 + f_{o3}k_3)$$

$$D_6 = Rh_1 + Rh_2(d_3 + h_{o3} + b_{o3}k_1 + d_{o3}k_2 + f_{o3}k_3) + Rh_3(d_2 + h_{o2} + b_{o2}k_1 + d_{o2}k_2 + f_{o2}k_3)$$

$$D_5 = R + k_p + Rh_1(d_3 + h_{o3} + b_{o3}k_1 + d_{o3}k_2 + f_{o3}k_3) + Rh_2(d_2 + h_{o2} + b_{o2}k_1 + d_{o2}k_2 + f_{o2}k_3) + Rh_3(d_1 + h_{o1} + b_{o1}k_1 + d_{o1}k_2 + f_{o1}k_3)$$

$$D_4 = (R + k_p)(d_3 + h_{o3} + b_{o3}k_1 + d_{o3}k_2 + f_{o3}k_3) + Rh_1(d_2 + h_{o2} + b_{o2}k_1 + d_{o2}k_2 + f_{o2}k_3) + Rh_2(d_1 + h_{o1} + b_{o1}k_1 + d_{o1}k_2 + f_{o1}k_3) + Rh_3(d_0 + h_{o0} + b_{o0}k_1 + d_{o0}k_2 + f_{o0}k_3)$$

$$D_3 = (R + k_p)(d_2 + h_{o2} + b_{o2}k_1 + d_{o2}k_2 + f_{o2}k_3) + Rh_1(d_1 + h_{o1} + b_{o1}k_1 + d_{o1}k_2 + f_{o1}k_3) + Rh_2(d_0 + h_{o0} + b_{o0}k_1 + d_{o0}k_2 + f_{o0}k_3)$$

$$D_2 = (R + k_p)(d_1 + h_{o1} + b_{o1}k_1 + d_{o1}k_2 + f_{o1}k_3) + Rh_1(d_0 + h_{o0} + b_{o0}k_1 + d_{o0}k_2 + f_{o0}k_3)$$

$$D_1 = (R + k_p)(d_0 + h_{o0} + b_{o0}k_1 + d_{o0}k_2 + f_{o0}k_3)$$

Where,

Published By:
Blue Eyes Intelligence Engineering
and Sciences Publication (BEIESP)

$h_3 = T_H T_T T_p$, $h_2 = T_H T_T + T_T T_p + T_H T_p$, $h_1 = T_H + T_T + T_p$

$a_{o3} = m_{11}$, $a_{o2} = d_3 m_{11} - d_0 m_{14}$, $a_{o1} = d_2 m_{11} - d_0 m_{13}$, $a_{o0} = d_1 m_{11} - d_0 m_{12}$

$c_{o3} = m_{21}$, $c_{o2} = d_3 m_{21} - d_0 m_{24}$, $c_{o1} = d_2 m_{21} - d_0 m_{23}$, $c_{o0} = d_1 m_{21} - d_0 m_{22}$

$e_{o3} = m_{31}$, $e_{o2} = d_3 m_{31} - d_0 m_{34}$, $e_{o1} = d_2 m_{31} - d_0 m_{33}$, $e_{o0} = d_1 m_{31} - d_0 m_{32}$

$g_{o3} = m_{41}$, $g_{o2} = d_3 m_{41} - d_0 m_{44}$, $g_{o1} = d_2 m_{41} - d_0 m_{43}$, $g_{o0} = d_1 m_{41} - d_0 m_{42}$

$b_{o3} = (m_{11}t_{11} + m_{12}t_{21} + m_{13}t_{31} + m_{14}t_{41})/T_H$, $d_{o3} = (m_{21}t_{11} + m_{22}t_{21} + m_{23}t_{31} + m_{24}t_{41})/T_H$

$f_{o3} = (m_{31}t_{11} + m_{32}t_{21} + m_{33}t_{31} + m_{34}t_{41})/T_H$, $h_{o3} = (m_{41}t_{11} + m_{42}t_{21} + m_{43}t_{31} + m_{44}t_{41})/T_H$

$b_{o2} = (m_{11}t_{21} + m_{12}t_{31} + m_{13}t_{41} - d_0 m_{14}t_{11} - d_1 m_{14}t_{21} + d_3 m_{11}t_{11} + d_3 m_{12}t_{21} - d_2 m_{14}t_{31} + d_3 m_{13}t_{31})/T_H$

$d_{o2} = (m_{21}t_{21} + m_{22}t_{31} + m_{23}t_{41} - d_0 m_{24}t_{11} - d_1 m_{24}t_{21} + d_3 m_{21}t_{11} + d_3 m_{22}t_{21} - d_2 m_{24}t_{31} + d_3 m_{23}t_{31})/T_H$

$f_{o2} = (m_{31}t_{21} + m_{32}t_{31} + m_{33}t_{41} - d_0 m_{34}t_{11} - d_1 m_{34}t_{21} + d_3 m_{31}t_{11} + d_3 m_{32}t_{21} - d_2 m_{34}t_{31} + d_3 m_{33}t_{31})/T_H$

$h_{o2} = (m_{41}t_{21} + m_{42}t_{31} + m_{43}t_{41} - d_0 m_{44}t_{11} - d_1 m_{44}t_{21} + d_3 m_{41}t_{11} + d_3 m_{42}t_{21} - d_2 m_{44}t_{31} + d_3 m_{43}t_{31})/T_H$

$b_{o1} = (m_{11}t_{31} + m_{12}t_{41} - d_0 m_{13}t_{11} - d_0 m_{14}t_{21} + d_2 m_{11}t_{11} - d_1 m_{13}t_{21} + d_2 m_{12}t_{21} - d_1 m_{14}t_{31} + d_3 m_{11}t_{21} + d_3 m_{12}t_{31})/T_H$

$d_{o1} = (m_{21}t_{31} + m_{22}t_{41} - d_0 m_{23}t_{11} - d_0 m_{24}t_{21} + d_2 m_{21}t_{11} - d_1 m_{23}t_{21} + d_2 m_{22}t_{21} - d_1 m_{24}t_{31} + d_3 m_{21}t_{21} + d_3 m_{22}t_{31})/T_H$

$f_{o1} = (m_{31}t_{31} + m_{32}t_{41} - d_0 m_{33}t_{11} - d_0 m_{34}t_{21} + d_2 m_{31}t_{11} - d_1 m_{33}t_{21} + d_2 m_{32}t_{21} - d_1 m_{34}t_{31} + d_3 m_{31}t_{21} + d_3 m_{32}t_{31})/T_H$

$h_{o1} = (m_{41}t_{31} + m_{42}t_{41} - d_0 m_{43}t_{11} - d_0 m_{44}t_{21} + d_2 m_{41}t_{11} - d_1 m_{43}t_{21} + d_2 m_{42}t_{21} - d_1 m_{44}t_{31} + d_3 m_{41}t_{21} + d_3 m_{42}t_{31})/T_H$

$b_{o0} = (m_{11}t_{41} - d_0 m_{12}t_{11} + d_1 m_{11}t_{11} - d_0 m_{13}t_{21} - d_0 m_{14}t_{31} + d_2 m_{11}t_{21} + d_3 m_{11}t_{31})/T_H$

$d_{o0} = (m_{21}t_{41} - d_0 m_{22}t_{11} + d_1 m_{21}t_{11} - d_0 m_{23}t_{21} - d_0 m_{24}t_{31} + d_2 m_{21}t_{21} + d_3 m_{21}t_{31})/T_H$

$f_{o0} = (m_{31}t_{41} - d_0 m_{32}t_{11} + d_1 m_{31}t_{11} - d_0 m_{33}t_{21} - d_0 m_{34}t_{31} + d_2 m_{31}t_{21} + d_3 m_{31}t_{31})/T_H$

$h_{o0} = (m_{41}t_{41} - d_0 m_{42}t_{11} + d_1 m_{41}t_{11} - d_0 m_{43}t_{21} - d_0 m_{44}t_{31} + d_2 m_{41}t_{21} + d_3 m_{41}t_{31})/T_H$

VII. SIMULATION AND RESULTS

With an objective to meet the specifications GM ≥ 6 dB, PM ≥ 40 degree and no frequency deviations in the steady-state, an extended state observer has been designed for the LFC model. A typical operating condition has been chosen as the nominal values of the parameters of the LFC model are shown in Table 1. A deviation of ± 10% on the nominal values of the parameters of LFC model has been considered for investigation of stability issues of the designed control scheme in Figure 4 for LFC model.

The closed-loop pole (CLP) locations have been chosen from the SRL plot for the equation (10) as shown in Figure 5. The closed-loop pole location is given by $s = -\rho_i$. With the help of three closed loop poles from SRL plot, feedback gain constants k_1, k_2 and k_3 are obtained using augmented state model.

The fourth-order extended observer has been designed with its pole locations are at seven times the controller pole locations (obtained from SRL plot) to determine D-matrix. The matrices T, G and M have been determined using Equations (6), (7) and (9) respectively. The open-loop transfer function $G_X(s)$ have been determined using equation (11) for stability margin analysis. Figure 6 indicates the variations in GM and PM at X with ρ for various values of ρ_i. It is observed that the GM and the PM remain almost constant with ρ in the higher range, but they vary appreciably with ρ_i. The critical PM occurs corresponds to loop opening at X.

In this paper, ρ=100 and ρ_i =9 have been selected to satisfy GM ≥ 6 dB and PM ≥ 40 degree. Table 2 shows the closed-loop pole locations and controller gains. The results of performance studies obtained by MATLAB simulations for the selected operating points are provided in Table 3 and 4. The results describing the disturbance rejection property for various load demand changes have been shown in Figure 7. The unit step response for frequency under parameter uncertainties is shown in Figure 8. Figure 9 shows the frequency deviations for the various load demands. That is, the control effort increases with increase in ΔP_D, thus for a certain higher value of ΔP_D, actuator can saturate [9].

Table 1: Area parameter values.

Area Parameter	R (puHz/Mw)	T_H (sec.)	T_T (sec.)	T_p (sec.)	K_p (puHz/Mw)
Nominal value	2.4	0.08	0.3	20	120
Nominal value +10%	2.64	0.088	0.33	20	90.91

Published By:
Blue Eyes Intelligence Engineering
and Sciences Publication (BEIESP)

Nominal value -10%	2.16	0.072	0.27	20	111.11

Table 2: Closed loop pole locations and associated gains.

CLP for	CLP locations	Observer poles	Controller gains
ρ=100 ρ_i =9	$\lambda_{2=}$ -16.23 $\lambda_{1=}$-7.28 +10.06i $\lambda_{0=}$-7.28 - 10.06i	r_3= −224.59 r_2 = −21079.06 r_1 = −1030522.95 r_0=−7724466.72	k_1 =1.19 k_2=7.14 k_3=9.51

Table 3: Result of frequency response studies on proposed system.

Loop break at X	Perturbation	GM (dB)	GCF (rad/sec)	PM (deg)	PCF (rad/sec)
	Nominal	8.13	87.3	41	34.8
	+10%	8.19	76.5	41.6	30.6
	-10%	8.29	90.2	41.5	35.5

Table 4: Settling time at varying load demands.

Load demand	Perturbation	Settling time (sec)	Maximum variation in frequency (Hz)
10%	Nominal	0.68	-5.38e-3
	+10%	0.81	-4.58e-3
	-10%	0.53	5.01e-3
20%	Nominal	0.69	-1.05e-3
	+10%	0.81	-9.19e-4
	-10%	0.53	9.85e-4

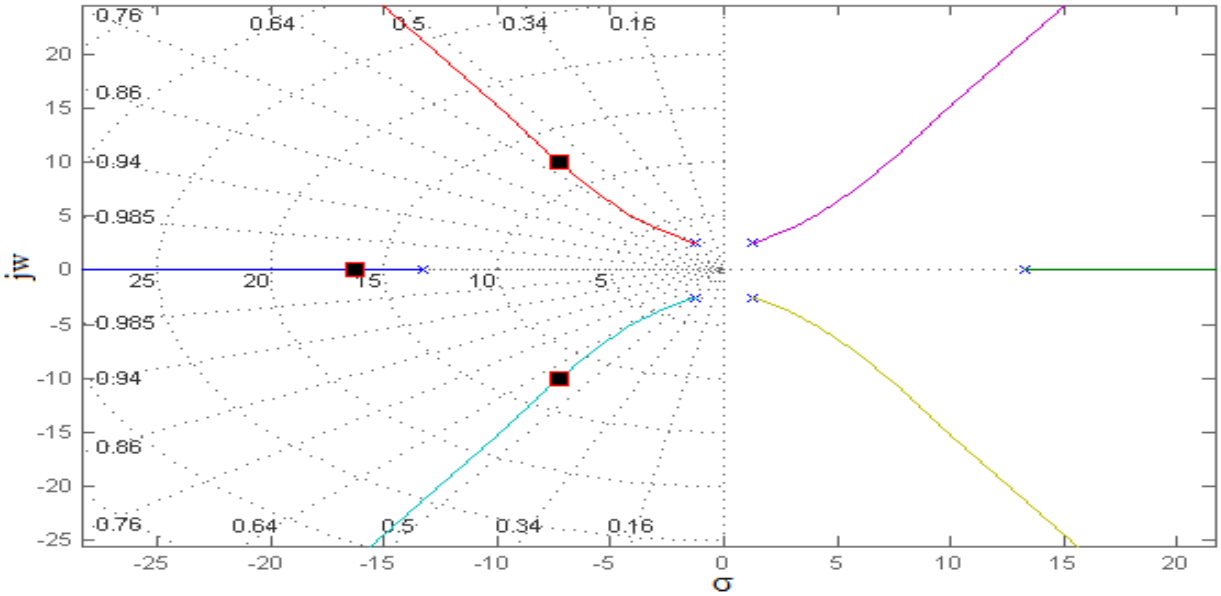

Figure 5: Symmetrical root locus diagram with selected closed-loop poles.

Published By:
Blue Eyes Intelligence Engineering
and Sciences Publication (BEIESP)

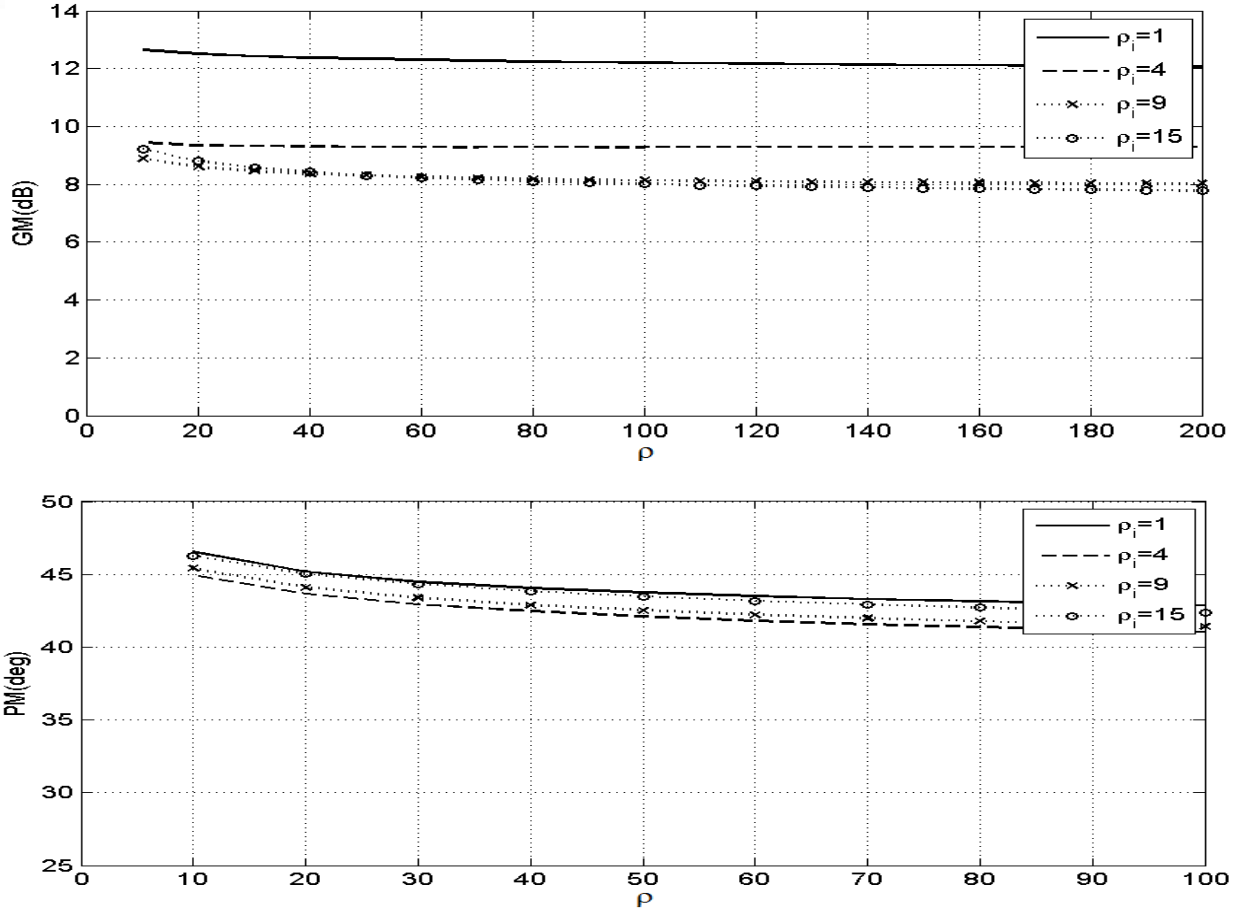

Figure 6: GM and PM of the open-loop system (11) as a function of ρ for various values of ρ_i.

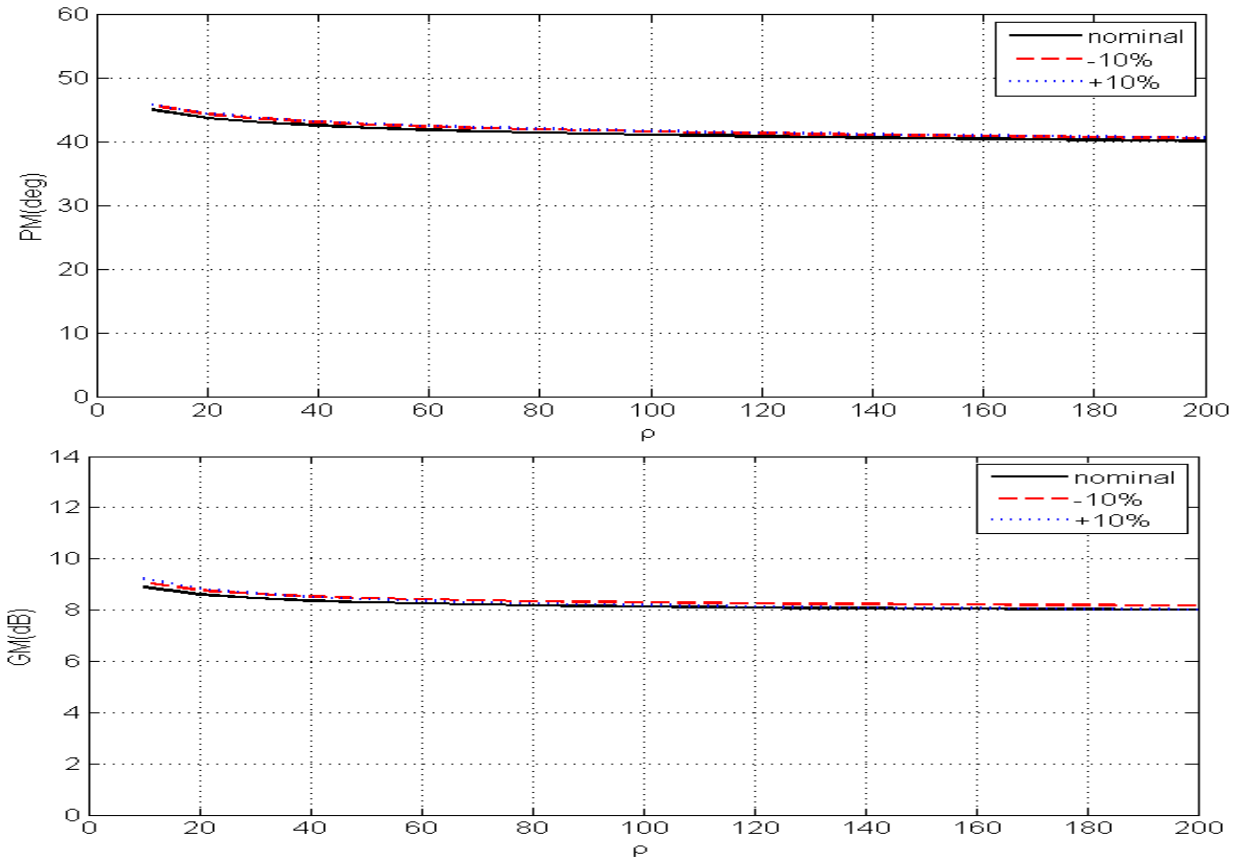

Figure 7: G M and PM as a function of ρ under parameter variations.

Published By:
Blue Eyes Intelligence Engineering
and Sciences Publication (BEIESP)

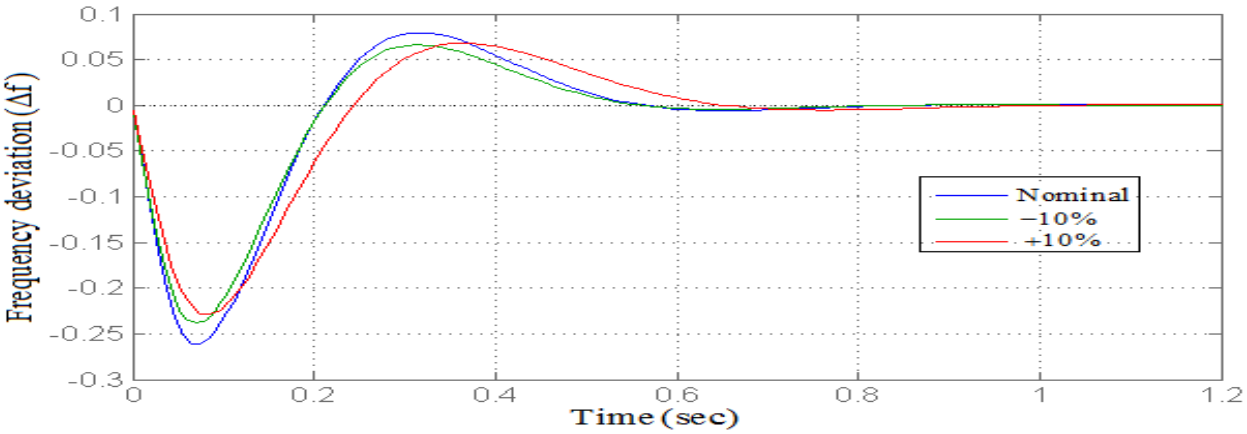

Figure 8:Unit step response under parameter uncertainties.

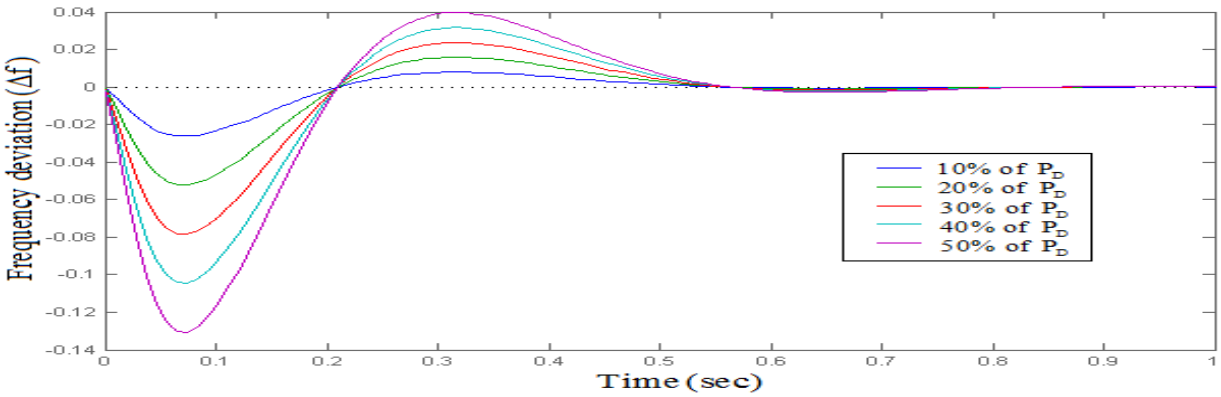

Figure 9: Dynamic response of system under varying values of load demands.

VIII. CONCLUSION

This paper presents a robust ESO-based load frequency controller for the single area power system subjected to bounded LFC loop parameter uncertainties as well as disturbances. The state-space ESO-based control technique is very effective to compensate input disturbances as well as perturbations in LFC parameters. The proposed approach shows that estimation of states and the parameter uncertainties plus external disturbances can be accomplished in an integrated manner using ESO. Implementation of full state feedback offers a scope for design trade-off between speed of response and the capabilities of hardware resources, assuring desired stability margins. It may be possible to fully utilize the capability of actuator, as the proposed method provides some control over peak values of Δf, ΔP_V and ΔP_T. The observer has been incorporated in terms of transfer functions in order to carry out stability analysis easily. The robust disturbance rejection capability and maintaining stability in the face of model parametric uncertainties have been demonstrated by a numerical example.

XI. NOTATIONS

r_0, r_1, r_2	roots of characteristic equation of extended reduced observer
$\lambda_0, \lambda_1, \lambda_2$	roots of characteristic equation of plant
ρ	system weighting penalty from SRL equation
ρ_i	weighting penalty assigned to system due to observer
u	control force/signal/input
T_s	settling time, s
T_H	hydraulic time constant, s
T_T	turbine time constant, s
T_P	generator/power system time constant, s
K_P	proportional gain of generator/power system, puHz/Mw
R	proportional speed regulation controller gain, puHz/Mw
w	disturbance
$K(k_1, k_2, k_3)$	feedback gains
e	error signal
s	Laplace variable
r	reference signal or set-point
H	per-unit inertia constant

Published By:
Blue Eyes Intelligence Engineering
and Sciences Publication (BEIESP)

REFERENCES

[1] Olle l. Elgerd, *Electric Energy Systems Theory; an introduction* (2nd Edition, McGraw-Hill Inc. 1982).
[2] K. Ogata, *Modern Control Engineering* (4th edition, Prentice Hall Inc. 2002).
[3] Gene F. Franklin, David Powell and Abbas Emami-Naeini, *Feedback Control of Dynamic Systems* (4th Edition, Pearsons Education Inc. 2002).
[4] S.K. Goswami and K.Datta, On estimation errors in linear systems due to parametric variations, *Journal of the institute of engineers (India), vol. 86, Dec. 2005, p(s) 192.*
[5] P. Kundur, *Power System Stability and Control* (McGraw Hill Inc. 1994).
[6] Prof. D.P. Kothari, Centre for Energy Studies on Automatic Generation Control, *IIT Delhi, Lecture 24.*
[7] R.K. Mehta, S.K. Goswami and K. Datta, An observer -based lateral autopilot for tail-controlled missiles, *IE(I) Journal-EL, Vol 88, sept. 2007, p(s): 17-22.*
[8] Dr. R.K. Mehta and Rittu Angu, An Observer-Based Robust Load Frequency Control, *proceeding on IOSR Journal of Electrical and Electronics Engineering (IOSR-JEEE) e-ISSN: 2278-1676,p-ISSN: 2320-3331, Volume 9, Issue 4 Ver. I (Jul – Aug. 2014), PP 23-31.*
[9] Rittu Angu and Dr. R.K. Mehta, Robust Stabilization of AVR Loop through Extended Reduced-Order Observer, *proceeding on International Journal of Emerging Science and Engineering (IJESE) ISSN: 2319–6378, Volume-3 Issue-2, December 2014.*

Rittu Angu was born in Aalo (Arunachal Pradesh), India, in 1987. He received his B-Tech in Electrical Engineering in 2010 and M-Tech in Power System Engineering in 2013 from NERIST (Deemed University), Nirjuli Itanagar, India. At present, he is pursuing his Ph.D. degree in the same university. His area of interest includes power system quality control and electrical machines and drives.

Dr. R. K. Mehta was born in Supaul (Bihar), India, in 1961. He received the B.Sc. Engg. degree in Electrical Engineering in 1987 and M.Tech. degree in Control Systems in 1992 from M.I.T., Muzaffarpur, (B.U.). He obtained his Ph.D. degree from Jadavpur University, Kolkata – 32. Currently he is working as Associate Professor, Department of Electrical Engineering, NERIST, Nirjuli, Arunachal Pradesh, India. His field of interest includes Missile Autopilot design, observer-based uncertainty and disturbance estimation and robust control.